# PULSE DESIGN METHODS FOR REDUCTION OF SPECIFIC ABSORPTION RATE IN PARALLEL RF EXCITATION

A. C. Zelinski[1], K. Setsompop[1], V. Alagappan[2], B. A. Gagoski[1], L. M. Angelone[2], G. Bonmassar[2], U. Fontius[3], F. Schmitt[3], E. Adalsteinsson[1,4], and L. L. Wald[2,4]

[1]Department of Electrical Engineering and Computer Science, MIT, Cambridge, MA, United States, [2]A. A. Martinos Center for Biomedical Imaging, Massachusetts General Hospital, Harvard Medical School, Charlestown, MA, United States, [3]Siemens Medical Solutions, Erlangen, Germany, [4]Harvard-MIT Division of Health Sciences and Technology, MIT, Cambridge, MA, United States

INTRODUCTION: A critical concern with multi-channel transmission is high specific absorption rate (SAR) due to the potential superposition of electric fields when using many simultaneous TX channels, and the possible inefficiency of producing excitation patterns via regional cancellation. To fully realize the clinical benefits of these systems, it is crucial to design RF pulses that not only achieve high-fidelity excitations, but ensure SAR falls within mandated limits. To explore this issue, we develop a method for calculating the SAR of an arbitrary RF pulse sequence on a parallel excitation system. Then we compare peak and average SAR due to three different RF pulse design methods: traditional singular value decomposition (SVD)-based inversion [1], Least Squares QR (LSQR) [2] and Conjugate Gradient Least Squares (CGLS) [3]. Calculating the SAR of each requires only an RF pulse set, knowledge of the steady state electric fields generated per unit of power sent to each TX coil, and knowledge of the tissue's electrical properties.

Figure 1: (a) 8-Channel Coil (b) Head Model
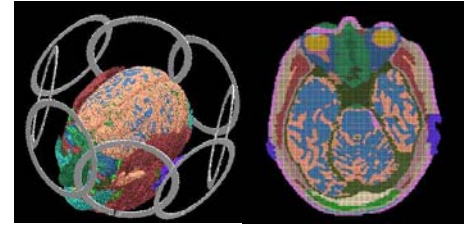
METHODS & RESULTS: **RF pulse design**. For a *P*-channel transmit system, linearizing and discretizing the nonlinear system of equations relating the RF waveforms played through each coil to the resulting excitation yields the linear system of equations **m=Ab** [4], where **m** is an Mx1 vector of target excitation samples in some region of interest, **b** is a voltage vector of the sampled RF waveforms played through each coil and **A** is an MxN matrix incorporating each coil's spatial sensitivity profile and the *k*-space trajectory. From **b**, samples of the RF pulse played along the *p*-th coil, $b_{1,p}(t)$, may be extracted.

Figure 2: SAR due to three RF designs (*R*=6)
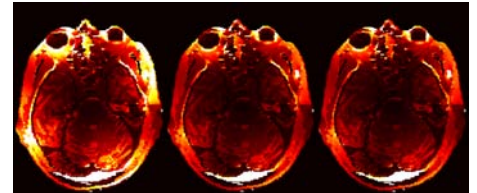
Solving m=Ab. For our experiment, the trajectory is a 2-D spiral whose rings are undersampled ("accelerated") by a factor of *R* relative to the field-of-view, and the target is an MIT logo. Furthermore, the spatial excitation field profiles for each coil in the 8-channel system (Siemens Magnetom TRIO, a TIM system) are known, so **m** and **A** are implicitly defined. For *R* = 1, 4, 6, 8, we compute **b** using the 3 methods, tuning the design parameters and peak voltage of each such that the flip angles of the resulting excitations are nearly equal (within 1-5%) when excited in a phantom on an 8-channel parallel TX array on a 3T Siemens Magnetom TRIO scanner [4]. For an equal or higher quality excitation, LSQR and CGLS yield $b_{1,p}(t)$ waveforms with significantly lower peak and root-mean-square (RMS) voltages than the SVD-based method [5].

Electric field calculation. Steady-state electric field distributions in a 29-tissue, high-resolution (1x1x2 mm^3) anatomically-accurate segmented head model are computed via finite difference time domain simulations of an 8-channel system at 7T [6], yielding the electric field at each spatial location *r* generated by each of the *P* coils: $\mathbf{E}_p(r,t)$. The 8-coil system and a slice of the head model are illustrated in **Figure 1**. The loop coil elements are 15-cm in diameter and the cylinder on which they are situated is 28-cm in diameter.

SAR calculation. Emulating Katscher et al.'s approach [7], the electric field and physical properties of the body at a fixed spatial location *r* generate $\mathrm{SAR}(r) = \sigma(r)(2\rho(r))^{-1}\left\langle\left\|\mathbf{E}(r)\right\|_2^2\right\rangle$, where $\langle\cdot\rangle$ is a time average, $\sigma(r)$ and $\rho(r)$ are the effective conductivity & mass density, respectively, and $\mathbf{E}(r,t)$ is the complex-valued 3-D electric field at time *t*. $\mathbf{E}(r,t) = \sum_{p=1}^{P} b_{1,p}(t)\mathbf{E}_p(r,t)$, i.e., the overall field at *t* is the linear superposition of the fields generated by each coil scaled by the pulse playing along each.

Peak and average SAR. For each RF design, SAR(*r*) in a 2-D slice of the head model is calculated, then average (whole-head) and peak SAR are computed, the latter being the peak in 2 mm^3 of tissue. **Figure 2** depicts SAR maps due to SVD-based, LSQR and CGLS waveforms when *R*=6; the latter two methods have lower SAR. **Figure 3** plots relative SAR values vs. *R*. For fixed *R*, the first two subplots clearly show that LSQR and CGLS generate significantly lower peak and mean SAR than the SVD-based method. The third subplot shows mean SAR's rapid growth with *R* (peak SAR also exhibits such rapid growth).

CONCLUSION: Branching away from traditional SVD-based inversion and using algorithms with favorable numerical properties (e.g., LSQR) led to markedly lower SAR while simultaneously achieving an equal-or-higher quality excitation. Furthermore, it was shown that average and peak SAR values exhibit rapid growth as a function of the *k*-space acceleration factor.

Figure 3: Relative SAR Performance